


## ORIGINAL ARTICLE

# Combined pre-conditioning with salidroside and hypoxia improves proliferation, migration and stress tolerance of adipose-derived stem cells

Yuan He<sup>1</sup> | Mudi Ma<sup>1,2</sup> | Yiguang Yan<sup>2</sup> | Can Chen<sup>1</sup> | Hui Luo<sup>3</sup> | Wei Lei<sup>1,2,3</sup> 

<sup>1</sup>Laboratory of Cardiovascular Diseases, Guangdong Medical University, Zhanjiang, China

<sup>2</sup>Cardiovascular Medicine Center, Affiliated Hospital of Guangdong Medical University, Zhanjiang, China

<sup>3</sup>Southern Marine Science and Engineering Guangdong Laboratory-Zhanjiang, The Marine Biomedical Research Institute, Guangdong Medical University, Zhanjiang, China

## Correspondence

Wei Lei, Laboratory of Cardiovascular Diseases, Guangdong Medical University, No. 57, Renmin Southern Road, Xiashan, Zhanjiang, Guangdong 524001, China.  
Email: leiwei2006@126.com

Hui Luo, The Marine Biomedical Research Institute, Guangdong Medical University, No. 2, Wenming Eastern Road, Xiashan, Zhanjiang, Guangdong 524001, China.  
Email: luohui@gdmu.edu.cn

Can Chen, Cardiovascular Medicine Center, Affiliated Hospital of Guangdong Medical University, No. 57, Renmin Southern Road, Xiashan, Zhanjiang, Guangdong 524001, China.  
Email: chencan-21@126.com

## Funding information

Natural Science Foundation of Guangdong Province, Grant/Award Number: 2019A1515011925; Competitive Key Scientific and Technological Program of Zhanjiang Municipal Financial Fund, Grant/Award Number: 2018A01023; Southern Marine Science and Engineering Guangdong Laboratory Zhanjiang, Grant/Award Number: ZJW-2019-07; Stem Cell Preclinical Research Projects of the Affiliated Hospital of Guangdong Medical University, Grant/Award Number: 2018PSSC004; Project of Guangdong Provincial Bureau of Traditional Chinese Medicine, Grant/Award Number: 20182068; National Natural Science Foundation of China, Grant/Award Number: 81700269 and 81970056

## Abstract

Oxidative stress after ischaemia impairs the function of transplanted stem cells. Increasing evidence has suggested that either salidroside (SAL) or hypoxia regulates growth of stem cells. However, the role of SAL in regulating function of hypoxia-pre-conditioned stem cells remains elusive. Thus, this study aimed to determine the effect of SAL and hypoxia pre-conditionings on the proliferation, migration and tolerance against oxidative stress in rat adipose-derived stem cells (rASCs). rASCs treated with SAL under normoxia (20% O<sub>2</sub>) or hypoxia (5% O<sub>2</sub>) were analysed for the cell viability, proliferation, migration and resistance against H<sub>2</sub>O<sub>2</sub>-induced oxidative stress. In addition, the activation of Akt, Erk1/2, LC3, NF-κB and apoptosis-associated pathways was assayed by Western blot. The results showed that SAL and hypoxia treatments synergistically enhanced the viability (fold) and proliferation of rASCs under non-stressed conditions in association with increased autophagic flux and activation of Akt, Erk1/2 and LC3. H<sub>2</sub>O<sub>2</sub>-induced oxidative stress, cytotoxicity, apoptosis, autophagic cell death and NF-κB activation were inhibited by SAL or hypoxia, and further attenuated by the combined SAL and hypoxia pre-treatment. The SAL and hypoxia pre-treatment also enhanced the proliferation and migration of rASCs under oxidative stress in association with Akt and Erk1/2 activation; however, the combined pre-treatment exhibited a more profound enhancement in the migration than proliferation. Our data suggest that SAL combined with hypoxia pre-conditioning may enhance the therapeutic capacity of ASCs in post-ischaemic repair.

## KEYWORDS

adipose-derived stem cells, hypoxia, oxidative stress, salidroside, stem cell function

This is an open access article under the terms of the Creative Commons Attribution License, which permits use, distribution and reproduction in any medium, provided the original work is properly cited.

© 2020 The Authors. *Journal of Cellular and Molecular Medicine* published by Foundation for Cellular and Molecular Medicine and John Wiley & Sons Ltd

## 1 | INTRODUCTION

Adipose-derived stem cells (ASCs) can be primarily harvested from adipose tissues by using a simple, minimally invasive method, and are easily cultured and expanded *in vitro*.<sup>1</sup> A number of studies have revealed that ASCs have multi-lineage potential as they can differentiate into multiple types of somatic cells, such as nerve cells, bone cells, endothelial cells and cardiomyocytes, under specific conditions.<sup>2,3</sup> Due to the cellular plasticity, ASCs are considered a promising cell source for regenerative medicine.

Transplantation of ASCs has been applied to the studies of post-ischaemic repair.<sup>4-6</sup> However, oxidative stress after ischaemia results in the production of reactive oxygen species (ROS) and inflammatory factors,<sup>7,8</sup> which can cause dysfunction of transplanted stem cells.<sup>9-11</sup> The accumulation of ROS also contributes to stem cell ageing and various types of cell death including apoptosis, necrosis and autophagic cell death (ACD; also known as type 2 programmed cell death [PCD]). Thus, enhancing the tolerance of ASCs against oxidative injury is critical to cell transplantation. Besides, generation of a sufficient number of transplanted cells can also increase the efficiency of post-implantation survival and proliferation capacity of stem cells *in vivo*.<sup>12</sup>

Autophagy is an evolutionarily conserved catabolic process that decomposes cytosolic proteins and organelles by forming autophagosomes to load cargo and subsequently fuse with lysosomes.<sup>13</sup> Accumulating evidence has demonstrated that autophagy plays a cytoprotective role in response to cellular stress. Specifically, Liu et al reported that autophagy actually promotes hypoxia pre-conditioning improving the viability of marrow mesenchymal stem cells (MSCs).<sup>14</sup> However, excessive autophagy may lead to ACD.<sup>15</sup> Several studies revealed that autophagy is involved in the regulatory mechanism of stem cell death and survival under stressed conditions.<sup>16-21</sup>

Hypoxia (1%-5% O<sub>2</sub>) pre-conditioning is a promising strategy to optimize or increase the self-renewal efficacy of MSCs, including bone marrow mesenchymal stem cells (BMSCs) and ASCs,<sup>22,23</sup> indicating that hypoxia pre-conditioning could be an approach to increase cell yield for clinical-scale ASC expansion. Moreover, hypoxia pre-conditioning enhances the survival of BMSCs in ischaemic tissues by increasing autophagy and decreasing apoptosis, suggesting that hypoxia may provide a protective effect on stressed injury in MSCs.<sup>14</sup> A similar stimulatory effect of hypoxia pre-conditioning was observed on BMSC survival *in vivo*, with about 5% of the transplanted BMSCs remaining alive on day 14, which implies that there is still a great room to improve stem cell function under stressed or pathological conditions. Salidroside (SAL) one of the main effective constituents of traditional Chinese herb *Rhodiola* possesses diverse pharmacological effects.<sup>25</sup> Indeed, SAL can promote the proliferation, differentiation, anti-apoptosis, anti-oxidation and anti-inflammation activities of MSCs.<sup>26-29</sup> Therefore, SAL may further enhance the function of hypoxia-pre-conditioned MSCs.

In this study, we determined the roles of SAL pre-conditioning on hypoxia-mediated proliferation and migration of rat ASCs (rASCs) by detecting the cell viability, cell proliferation, migratory ability

and the activation of Akt, Erk1/2 and LC3. Furthermore, we also determined whether H<sub>2</sub>O<sub>2</sub>-mediated cytotoxicity, cell death, redox disequilibrium and NF- $\kappa$ B activation contribute to the resistance of pre-conditioned rASCs against oxidative stress.

## 2 | MATERIALS AND METHODS

### 2.1 | Culture, identification and transfection of rASCs

rASCs were purchased from Cyagen Biosciences Inc. rASCs were planted in a 75-cm<sup>2</sup> culture flask and maintained in basal medium, supplemented with 10% foetal bovine serum, 2 mmol/L glutamine and 1% penicillin-streptomycin solution. The cells were incubated in a humidified incubator with 5% CO<sub>2</sub> at 37°C. The culture media were changed every two days, and the adherent cells were passaged at a confluency of approximately 80%.

P5-7 rASCs used in this study were identified by immunophenotyping and directed differentiation of specific lineages. rASCs for immunophenotyping by flow cytometry (FCM) were digested and resuspended in 100  $\mu$ L antibody working solution (90  $\mu$ L of PBS containing 5% FBS and 10  $\mu$ L of fluorescein-conjugated monoclonal antibody or isotype control). The antibodies and isotype controls used for immunophenotyping were as follows: PE hamster anti-rat CD29, PE hamster IgM, PE mouse anti-rat CD45 and PE mouse IgG1, from BD Bioscience; CD90 monoclonal antibody (OX-7), PE and CD34 monoclonal antibody (QBEND/10), PE, from Thermo Fisher Scientific. After being incubated in the dark on ice with shaking for 1 hour, rASCs were washed 3 times with PBS and then analysed by FCM. rASCs for osteogenic and adipogenic differentiation were cultured in 6-well plates and orientatedly induced using osteogenic differentiation medium and adipogenic differentiation medium, respectively. After the induction of differentiation, rASCs were stained with Alizarin red or Oil Red O and observed under an inverted phase-contrast microscope (Leica, DMI3000 B).

The lentivirus (LV) for *stubRFP-sensGFP-LC3* overexpression was purchased from GeneChem. Cell transfection was performed following the protocol provided by the manufacturer. Polybrene (5  $\mu$ g/mL) was added to the medium for improving transfection efficiency.

### 2.2 | SAL and hypoxia pre-conditionings

rASCs in the logarithmic growth phase were seeded in cell culture plates at a density of  $3 \times 10^3$ /well, followed by serum deprivation for 24 hours when cells reached confluence of 50%-60%. In order to explore the most optimal pre-conditioning conditions, rASCs were incubated at 37°C with different concentration of SAL (0, 25, 50, 100, 200 and 400  $\mu$ mol/L, respectively) in a 5% CO<sub>2</sub> incubator (Thermo Fisher Scientific, 371, USA) or in a tri-gas incubator (Thermo Fisher Scientific, 3131, USA) that maintains a 5% O<sub>2</sub> level. rASCs were pre-conditioned for 1, 3 and 5 days.

### 2.3 | Cell viability analysis

The cell viability was measured using an enhanced Cell Counting Kit-8 (CCK-8, Beyotime). Briefly, 100  $\mu\text{L}$  CCK-8 solution was added to each well. After 2 hours of incubation at 37°C, the optical density (OD) value was measured at  $A_{450}$  nm. Three independent experiments were run.

### 2.4 | Cell proliferation detection

Cell proliferation was assessed by detection of BrdU incorporation. BrdU can be inserted into the DNA chain which is replicating and thus may be used as a measure of cell proliferation. Cells grown on 13-mm round coverslips were incubated with a final concentration of 10  $\mu\text{mol/L}$  of BrdU (5-bromo-2'-deoxyuridine). After 1 hour of culture, cells were fixed with 4% paraformaldehyde for 30 minutes at room temperature. The coverslips were washed with PBS and then incubated for 30 minutes with 0.1% Triton X-100 to permeabilize the membranes. Cultures were incubated with 1 mol/L HCl for 10 minutes on ice, 2 mol/L HCl for 10 minutes at room temperature and with 2 mol/L HCl for 20 minutes at 37°C. After DNA denaturation, cells were incubated with 0.1 mol/L sodium-borate buffer, pH 8.4, for 12 minutes at room temperature, then washed three times with 0.1% Triton X-100, blocked with 2% BSA in PBS for 1 hour at room temperature and incubated with anti-BrdU antibodies (Cell Signaling Technology, CST) overnight at 4°C. After being washed with PBS, cells were incubated with secondary antibody (anti-mouse IgG, Alexa Fluor 488 Conjugate, CST) at a 1:500 dilution for 1 hour at 37°C. Finally, the cell nuclei were stained with DAPI (4',6'-diamidino-2-phenylindole). Each coverslip was observed using a laser scanning confocal microscope (Leica, TCS SP5 II) and then analysed by counting, in a blind fashion. The BrdU-positive cells and total cells in five viewing fields were counted under a 20 $\times$  objective microscope.

### 2.5 | Observation of autophagosomes and autolysosomes

rASCs transfected with *stubRFP-sensGFP-LC3* LV were seeded in 30-mm glass-bottom culture dishes. At the end of the experiments, rASCs were observed under a laser scanning confocal microscope (LSCM, Leica). The fluorescence of yellow dots (overlays of red and green channels) and red dots was observed in five viewing fields, and was counted manually by a person unfamiliar with this study. The number of autophagosomes and autolysosomes in each cell was calculated as the yellow dots and red dot, respectively.

### 2.6 | Oxidative stress induced by hydrogen peroxide ( $\text{H}_2\text{O}_2$ ) and cytotoxicity assay

Oxidative stress was induced by addition of  $\text{H}_2\text{O}_2$  (400  $\mu\text{mol/L}$ ) in low-glucose DMEM (Dulbecco's modified Eagle medium) supplemented

with 0.1% FBS. We first performed LDH release assay to analyse  $\text{H}_2\text{O}_2$ -mediated cytotoxicity. The destruction of plasma structure caused by cell death results in the release of enzymes in cytoplasm into the culture medium, including LDH, which has relatively stable enzymatic activity. LDH release was analysed using a LDH Cytotoxicity Assay Kit (Beyotime, Shanghai, China). After  $\text{H}_2\text{O}_2$  treatment for 24 hours, the cell culture plates were centrifuged for 5 minutes at 400 g. Cell culture supernatant (120  $\mu\text{L}$ /well) was transferred from each well to 96-well culture plates. Cells were washed once with PBS and incubated with 150  $\mu\text{L}$  LDH release reagent (1:10 dilution) at 37°C for 1 hour; then, the supernatants were also transfer to a new culture plate. 60  $\mu\text{L}$  LDH test solution was added to the transferred supernatant. The plate was incubated at room temperature (22-25°C) in the dark for 30 minutes. Finally, the absorbances were read at 490 nm using a microplate spectrophotometer (Epoch, BioTek). The percentage of LDH release was calculated using the following formula:

$$\text{LDH release(\%)} = \frac{\text{LDH in supernatant}}{\text{LDH in supernatant} + \text{intracellular LDH}} \times 100.$$

### 2.7 | Cell apoptosis assay

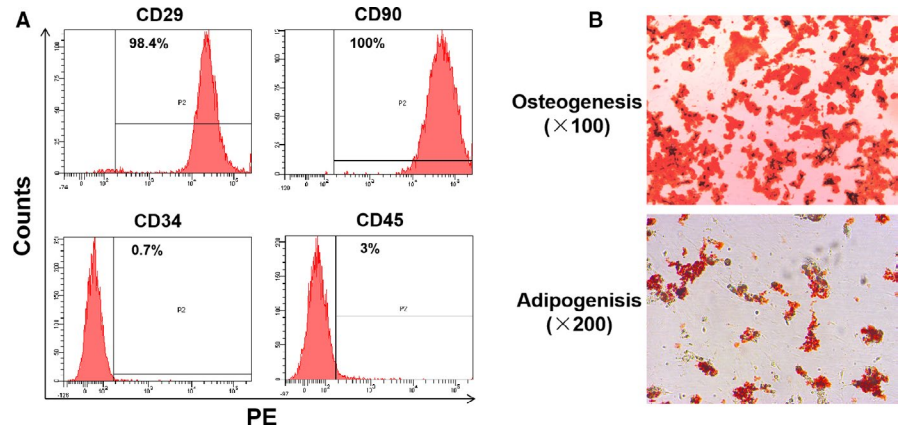
After being incubated with  $\text{H}_2\text{O}_2$  or PBS for 24 hours, cells were fixed with 4% paraformaldehyde at room temperature for 30 minutes. In Situ Cell Death Detection Kit (Roche) was used for TUNEL staining. Briefly, cells were incubated in a 0.1% Triton-100 solution and then incubated with a TUNEL reaction mixture. Finally, nuclei were stained with 1  $\mu\text{g/mL}$  DAPI. Besides, apoptosis was also detected using the Annexin-V-FITC Apoptosis Detection Kit (BD Pharmingen). The protocol was performed in accordance with the manufacturer's instructions. Cells were digested into single cell suspensions with EDTA-free trypsin and then subjected to the Annexin V/PI. The stained cells were analysed by FCM in one hour after staining.

### 2.8 | Malondialdehyde (MDA) and glutathione (GSH) measurement

The contents of MDA and GSH were respectively measured using a Lipid Peroxidation MDA Assay Kit and a Total Glutathione Assay Kit (Beyotime), according to the manufacturer's instruction. Cells were homogenized with PBS, and the homogenate was centrifuged at 10 000 g for 10 minutes. The supernatant was taken for the subsequent measurement.

For MDA measurement, 0.1 mL homogenate or standards were added to a tube, and subsequently 0.2 mL MDA test working solution was added. The mixture was heated in boiling water bath for 15 minutes, then cooled to room temperature and centrifuged at 1,000 g for 10 minutes. 200  $\mu\text{L}$  supernatant was added to a 96-well plate, and then, the absorbance at 532 nm was measured using a microplate spectrophotometer. For GSH measurement, 10  $\mu\text{L}$  homogenate or standards, 10  $\mu\text{L}$  protein removal reagent S solution and 150  $\mu\text{L}$  total glutathione detection working solution were sequentially

**FIGURE 1** Characterization of P5-7 rASCs. Cluster of differentiation (CD) profile of rASCs was analysed by FCM prior to treatments (A). Osteogenic-induced and adipogenic-induced rASCs were stained with Alizarin red and Oil Red O, respectively (B)



added to each well of a 96-well plate, then mixed and incubated at room temperature for 5 minutes. 50  $\mu$ L NADPH solution (0.5 mg/mL) was added to each well. After mixing, the absorbance at 412 nm was measured every 5 minutes for a total of 25 minutes. MDA or GSH content was calculated according to the standard curve.

## 2.9 | Catalase (CAT) activity assay

CAT (EC 1.11.1.6) activities were determined using a Catalase Assay Kit (Beyotime), following the manufacturer's protocols, as previously described.<sup>30</sup> Cells were lysed with Cell lysis buffer for Western and IP (Beyotime), and then, the cell lysates were diluted with catalase assay buffer. 40  $\mu$ L supernatants were mixed with 10  $\mu$ L catalase assay buffer containing 250 mmol/L  $H_2O_2$ . After incubation at 25°C for 3 minutes, 450  $\mu$ L of reaction termination buffer was added to stop the reaction. A total of 10  $\mu$ L of the mixtures were diluted 5-fold with the catalase assay buffer. Subsequently, 10  $\mu$ L of the diluted mixtures was added into a 96-well plate and incubated with 200  $\mu$ L of working colour reagent for 20 minutes. Finally, the absorbance was measured at 520 nm by a microplate spectrophotometer (Epoch, BioTek). CAT activity was calculated and expressed as U/mg protein.

## 2.10 | Cell migration assay

Transwell migration assay was performed using Transwell chambers with 8- $\mu$ m filter inserts (BD Pharmingen). Cells were trypsinized and suspended in medium with 0.5% FBS. Then, cells (30 000 cells/cm<sup>2</sup>) were seeded in the top of the inserts and placed in the wells containing medium with 10% FBS. After incubating the cells for 12 hours at 37°C, the inserts were washed with PBS twice and cells on the upper surface of the inserts were gently removed with a cotton swab. The Transwell filters were fixed with 4% paraformaldehyde for 30 minutes, rinsed with ultra-pure water and stained with 0.1% crystal violet for 20 minutes. The cells that had migrated to the lower surface were visualized and photographed under an inverted microscope (Leica). The migration rate was analysed using the Image-Pro Plus 6.0 software.

## 2.11 | Western blot

Cells were lysed with RIPA Buffer. Protein concentration was determined using the BCA method. Briefly, proteins (15  $\mu$ g) were denatured and separated by 10% SDS-PAGE gels and electroblotted onto PVDF membranes. The membranes were incubated with anti- $\beta$ -actin (1:1000), anti-Akt (1:2000), anti-p-Akt (Ser473, 1:2000), anti-Erk1/2 (1:1000), anti-p-Erk1/2 (Thr202/Try204, 1:1000), anti-LC3A/B (1:1000), anti-NF- $\kappa$ B-p65 (1:1000), anti-p-NF- $\kappa$ B-p65 (Ser536, 1:1000), anti-p38MAPK (1:1000), anti-p-p38MAPK (1:1000), anti-caspase-9 (1:1000), anti-cleaved-caspase-9 (1:500), anti-Bcl-2 (1:1000) and anti-Bax (1:1000) antibodies (CST) for at least 16 hours at 4°C. The goat anti-rabbit IgG (1:2000, CST) was incubated at room temperature for 1 hour as the secondary antibody. Immunoreactions were detected using an electrochemiluminescence (ECL) system according to the manufacturer's instructions. The grey value was calculated by the ImageJ analysis software (National Institutes of Health, USA).

## 2.12 | Statistical analysis

Data were expressed as mean  $\pm$  SEM for the values obtained from three independent experiments. Statistical analyses were performed by analysis of variance (ANOVA) followed by the Bonferroni multiple comparison test (GraphPad Prism 5.0). A *P*-value < 0.05 was considered statistically significant.

## 3 | RESULTS

### 3.1 | SAL and hypoxia pre-conditionings synergistically promote cell proliferation and autophagic flux in rASCs under non-stressed conditions

rASCs were characterized for antigens (Figure 1A) and induction of differentiation (Figure 1B). We first determined the effects of time cause of hypoxia and the dose response of SAL on cell

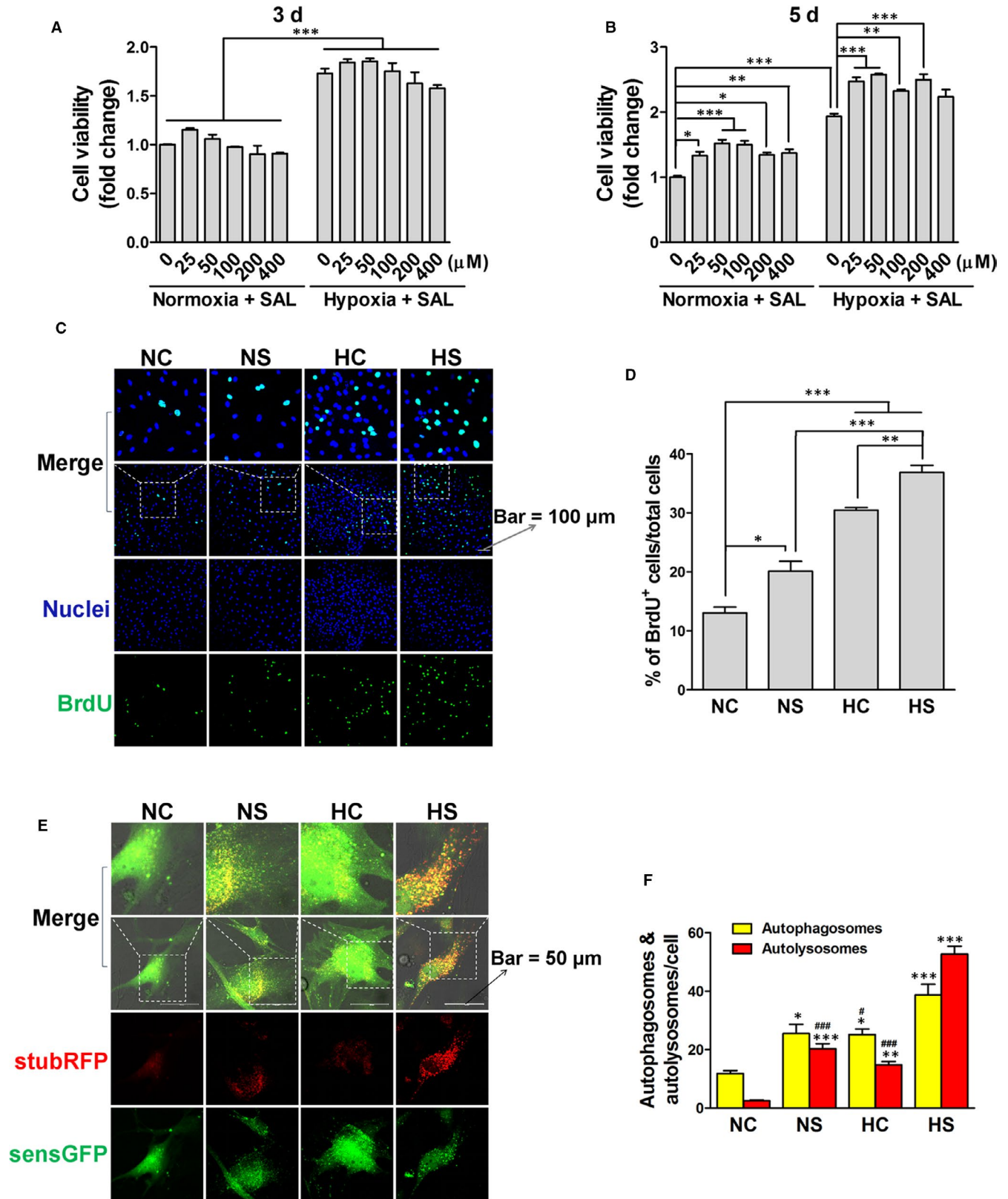
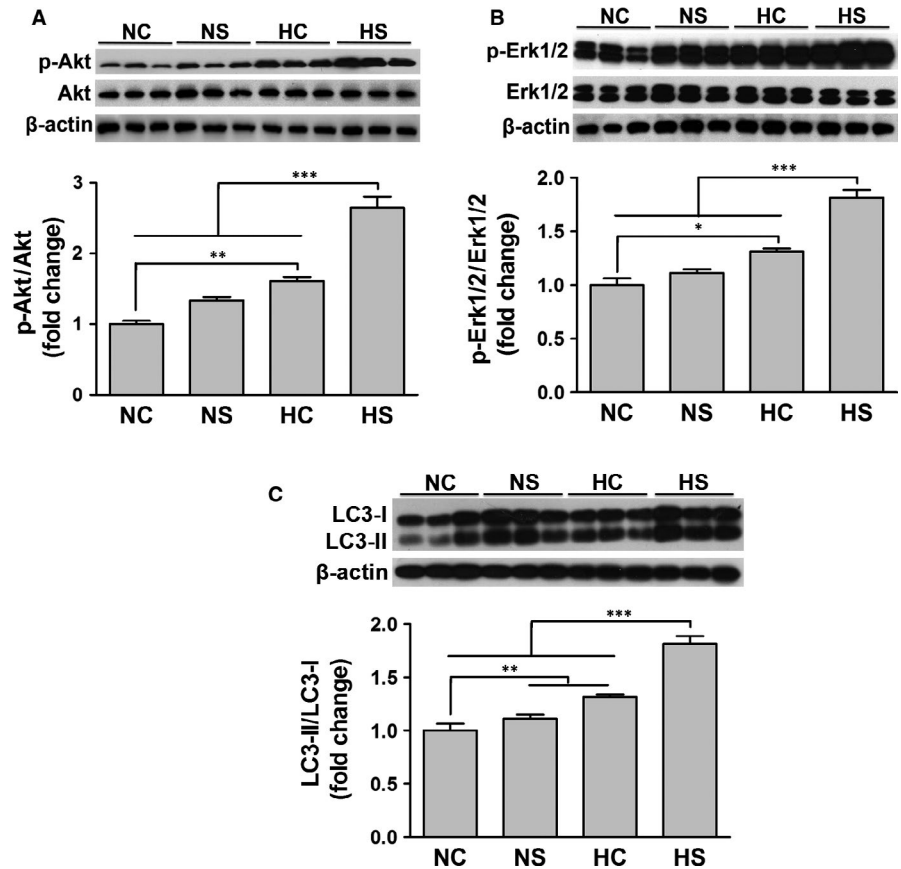


**FIGURE 2** Effects of SAL and hypoxia treatments on cell viability, proliferation and autophagy. After the treatment with SAL (25–400 μmol/L), hypoxia or hypoxia + SAL (25–400 μmol/L), the cell viability of rASCs was determined by CCK-8 assay on day 3 (A) and day 5 (B). Then, rASCs were treated with normoxia + DMSO (NC), normoxia + 50 μmol/L SAL (NS), hypoxia + DMSO (HC) or hypoxia + 50 μmol/L SAL (HS). After being treated for 5 days, the cell proliferation was analysed by BrdU incorporation assay (C and D), and the autophagic flux was assessed by stubRFP-sensGFP-LC3 (E and F). \**P* < .05, \*\**P* < .01, \*\*\**P* < .001 (A, B and D). \**P* < .05 vs NC, \*\**P* < .01 vs NC, \*\*\**P* < .001 vs NC, #*P* < .05 vs HS, ###*P* < .001 vs HS (F)

**FIGURE 3** Effects of SAL and hypoxia treatments on Akt, Erk1/2 and LC3 activation. The phosphorylation levels of Akt (A) and Erk1/2 (B) and the ratio of LC3-II/LC3-I (C) were analysed by Western blot. \* $P < .05$ , \*\* $P < .01$ , \*\*\* $P < .001$



viability of rASCs. Vehicle treatment under normoxia was used as a control. CCK-8 assay results showed that hypoxia treatment for at least 3, but not 1 days (data not shown) significantly increased cell viability (Figure 2A,B). However, SAL did not show significant effects until day 5. Taken together, SAL at a concentration of 50  $\mu\text{mol/L}$  had the most robust effects on cell viability under normoxia and hypoxia.

Based on the results of CCK-8 assay, rASCs were treated and grouped as follows: NC group (normoxia + DMSO), NS group (normoxia + 50  $\mu\text{mol/L}$  SAL), HC group (hypoxia + DMSO) and HS group (hypoxia + 50  $\mu\text{mol/L}$  SAL). Cells in each group were treated for 5 days. The cell proliferation of rASCs was determined by the BrdU incorporation assay. To examine the status of autophagy, rASCs were transfected with *stubRFP-sensGFP-LC3* LV and monitored under the oil microscope. As shown in Figure 2C-F, the NS, HC and HS groups displayed significant increases in the number of BrdU + cells and autophagosomes/autolysosomes, compared to the NC group. Moreover, the HS treatment showed synergistic effects in promoting proliferation and autophagic flux in rASCs.

The expression of Akt, p-Akt, Erk1/2, p-Erk1/2 and LC3 was determined by Western blot. p-Akt and p-Erk1/2 levels were presented as the ratio of phosphorylated to total proteins. As shown in HC or HS, but not NS significant increased p-Akt and p-Erk1/2 (Figure 3A,B). NS, HC and HS increased the ratio of LC3-II/LC3-I (Figure 3C). Moreover, HS led to higher levels of p-Akt, p-Erk1/2 and LC3-II/LC3-I, compared with NS and HC. These findings indicate that SAL and hypoxia pre-conditionings promote the proliferation of rASCs under non-stressed conditions in association with enhanced autophagic activity and activation of Akt, Erk1/2 and LC3.

### 3.2 | SAL and hypoxia pre-conditionings synergistically attenuate $\text{H}_2\text{O}_2$ -mediated cell death

To investigate whether SAL and hypoxia pre-conditionings have protective effects against oxidative injury, rASCs were treated with PBS or  $\text{H}_2\text{O}_2$  following the NC (normoxia + DMSO), NS (normoxia + 50  $\mu\text{mol/L}$  SAL), HC (hypoxia + DMSO) and HS

**FIGURE 4** Protective effects of SAL and hypoxia pre-treatments against  $\text{H}_2\text{O}_2$ -mediated cell death. The cytotoxicity was determined by LDH release assay (A). The cell apoptosis was analysed by Annexin V-FITC/PI-double staining (B). The apoptosis rate was measured by calculating the percentage of late-stage apoptotic cells (C). The apoptosis was further confirmed by TUNEL assay (D). The autophagosomes and autolysosomes were measured by *stubRFP-sensGFP-LC3* (E), and their numbers were counted under a laser confocal microscope (F). \* $P < .05$ , \*\* $P < .01$ , \*\*\* $P < .001$  (A and C). \*\* $P < .01$  vs NC + PBS, \*\*\* $P < .001$  vs NC + PBS, # $P < .05$  vs NC +  $\text{H}_2\text{O}_2$ , ### $P < .01$  vs NC +  $\text{H}_2\text{O}_2$ , #### $P < .001$  vs NC +  $\text{H}_2\text{O}_2$  (F)

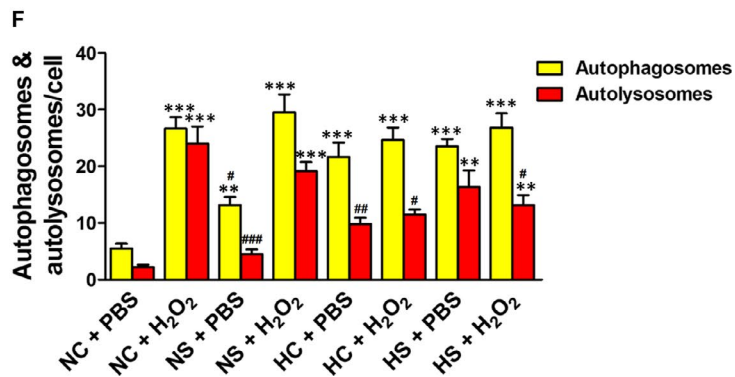
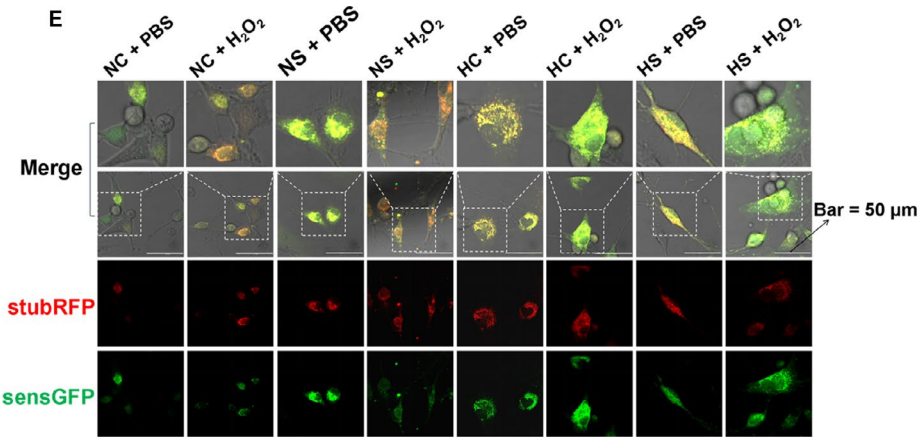
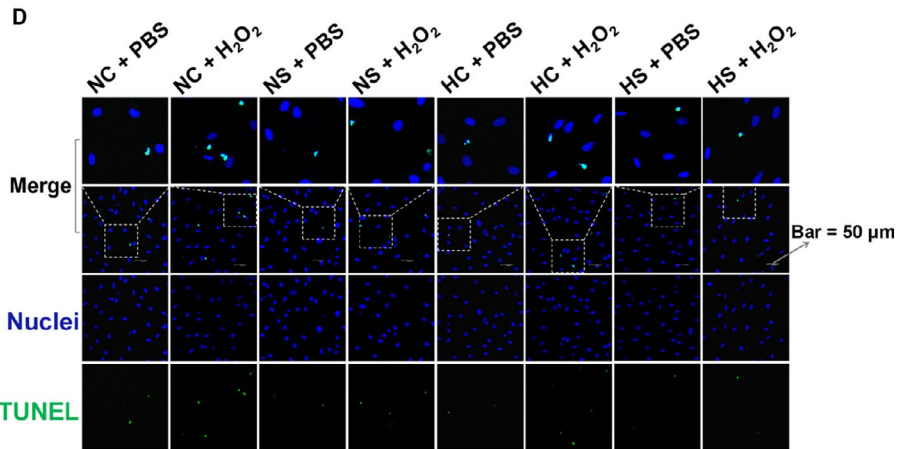
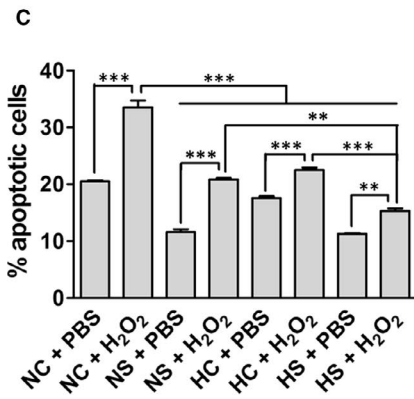
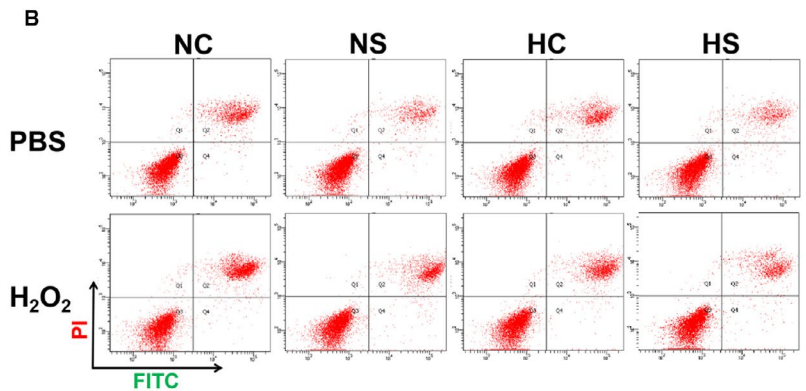
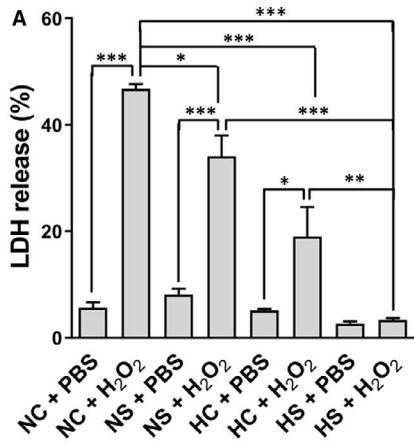
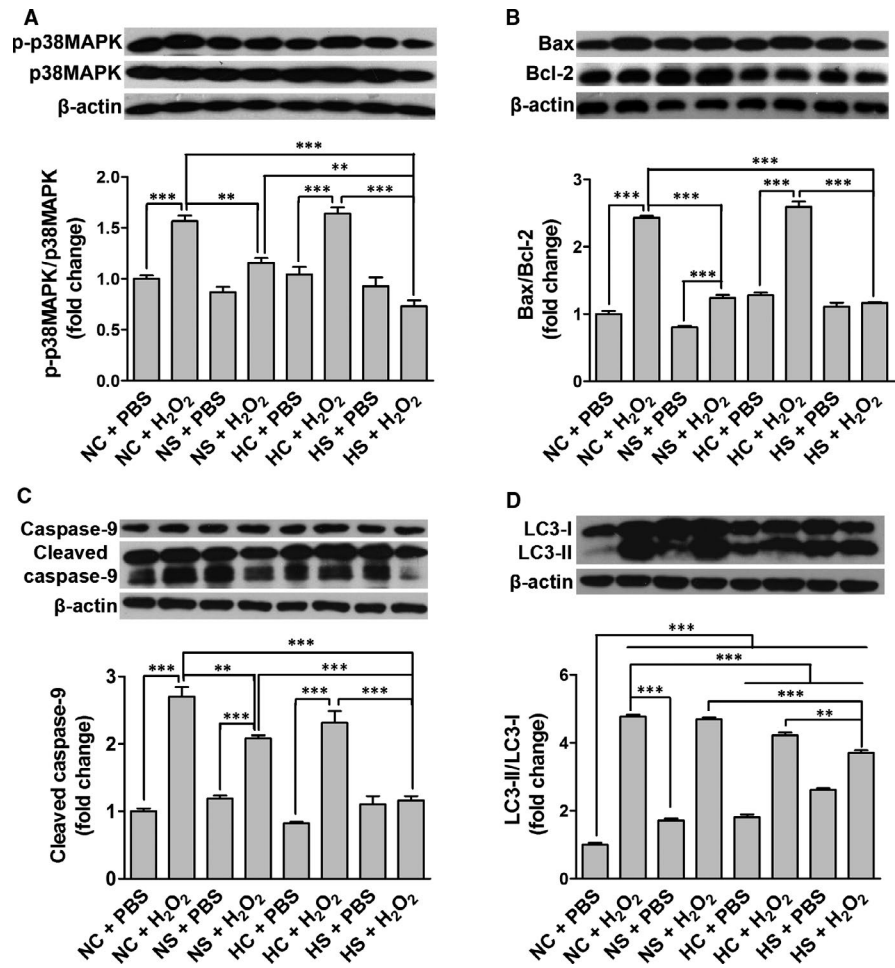


**FIGURE 5** Effects SAL and hypoxia pre-treatments on  $H_2O_2$ -induced activation of apoptosis pathways and LC3. The levels of p38MAPK phosphorylation (A), Bax/Bcl-2 (B), caspase-9 cleavage (C) and LC3-II/LC3-I (D) of rASCs were determined by Western blot, after the  $H_2O_2$  treatment following the NC, NS, HC or HS pre-treatment. \*\* $P < .01$ , \*\*\* $P < .001$



(hypoxia + 50  $\mu\text{mol/L}$  SAL) pre-treatment. LDH release is an important indicator of cell membrane integrity and is widely used for cytotoxicity testing. As shown in Figure 4A, the NC +  $H_2O_2$  group exhibited  $46.8 \pm 0.86\%$  of LDH release, which was significant higher than found in the other groups. The NS, HC and HS pre-treatments reversed LDH release caused by  $H_2O_2$  treatment, and HS pre-treatment showed a synergistic effect.

$H_2O_2$ -induced apoptosis was analysed by FCM. The NC pre-treatment followed by the PBS treatment induced a significantly higher apoptosis, while the  $H_2O_2$  treatment significantly induced a higher apoptosis rate ( $33.6 \pm 1.62\%$ ) (Figure 4B,C). The NS and HC pre-treatments obviously attenuated  $H_2O_2$ -induced apoptosis, and the protective effects were enhanced by the HS pre-treatment. The FCM results suggesting apoptosis were confirmed by TUNEL staining (Figure 4D). Autophagy activation in response to  $H_2O_2$  stimulation was evaluated by investigating the numbers of autophagosomes and autolysosomes. We found the NC pre-treatment followed by the  $H_2O_2$  treatment resulted in significantly increased formation of autophagosomes/autolysosomes compared to the NC + PBS group, while the HC and HS pre-treatments markedly inhibited autolysosome formation induced by  $H_2O_2$  (Figure 4E,F).

To further verify the changes in cell apoptosis and autophagy, we performed Western blot to detect the ratio of Bax/Bcl-2 and

LC3-II/LC3-I and the levels of p-p38MAPK and cleaved caspase-9. We observed that p-p38MAPK, Bax/Bcl-2, cleaved caspase-9 and LC3-II/LC3-I were significantly up-regulated in the NC +  $H_2O_2$  group, compared to the NC + PBS group (Figure 5A-D). The NS and HS pre-treatments significantly decreased the ratio of Bax/Bcl-2 and the levels of p-p38MAPK and cleaved caspase-9, while the HC and HS pre-treatments reduced the ratio of LC3-II/LC3-I (Figure 5A-D).

Collectively, these results demonstrate that SAL and hypoxia pre-conditionings synergistically attenuate  $H_2O_2$ -mediated cell death partly by protecting rASCs against apoptosis and ACD.

### 3.3 | SAL and hypoxia pre-conditionings synergistically inhibit $H_2O_2$ -induced oxidative stress and NF- $\kappa$ B activation

MDA is a natural product of lipid oxidation in organisms. Lipid oxidation occurs when oxidative stress occurs in animal or plant cells. After oxidation, fatty acids can be gradually decomposed into a series of complex compounds including MDA. Thus, the level of lipid oxidation can be accessed by detecting MDA content. GSH and CAT, the important endogenous antioxidants, can provide protection against oxidative stress by removing excessive peroxides.



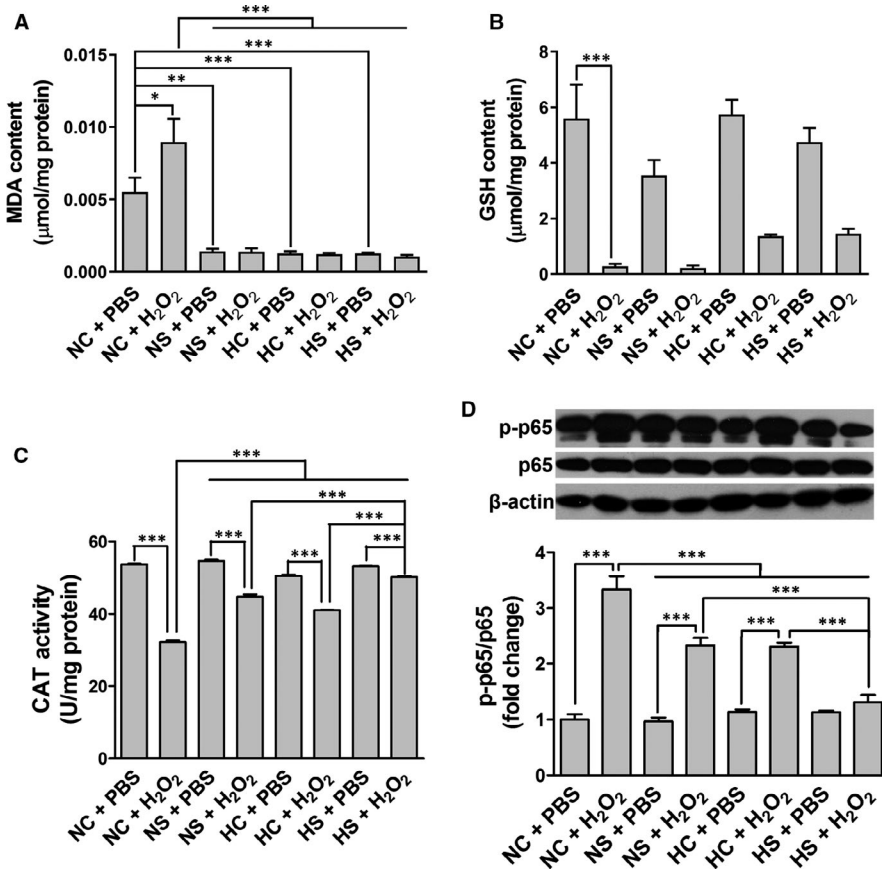


**FIGURE 6** Effects of SAL and hypoxia pre-treatments on H<sub>2</sub>O<sub>2</sub>-induced oxidative stress and NF-κB activation. The contents of MDA (A) and GSH (B) and the enzymatic activity of CAT (C) were quantitated in the extracts of rASCs using the colorimetric method. NF-κB-p65 phosphorylation (D) of rASCs was determined by Western blot. \**P* < .05, \*\*\**P* < .001

The contents of MDA and GSH and the enzymatic activity of CAT were quantitated in the extracts of rASCs using the colorimetric method. It is found that the level of MDA was significantly up-regulated in the NC + H<sub>2</sub>O<sub>2</sub> group compared to other groups, suggesting that SAL and hypoxia pre-conditionings had favourable effects on lightening lipid hyperoxidation induced by H<sub>2</sub>O<sub>2</sub> (Figure 6A). As shown in Figure 6B,C, 24 hours of the H<sub>2</sub>O<sub>2</sub> treatment resulted in significant reduction of GSH content and CAT enzymatic activities, while the NS, HC and HS pre-treatments alleviated the CAT inactivation induced by H<sub>2</sub>O<sub>2</sub>, but showed no significant effects on GSH. Importantly, after the HS pre-treatment followed by the H<sub>2</sub>O<sub>2</sub> treatment, the changes in CAT enzyme activities showed a higher level than those in the NS + H<sub>2</sub>O<sub>2</sub> and HC + H<sub>2</sub>O<sub>2</sub> groups.

NF-κB activation in response to H<sub>2</sub>O<sub>2</sub> stimulation was evaluated by investigating the phosphorylation of NF-κB P65. The results of Western blot showed that the H<sub>2</sub>O<sub>2</sub> treatment significantly increased p-NF-κB p65 compared with the PBS treatment, after the NC, NS or HC pre-treatment (Figure 6D). Compared with the NC + H<sub>2</sub>O<sub>2</sub> group, rASCs pre-treated with NS, HC or HS following by the H<sub>2</sub>O<sub>2</sub> treatment showed significant decreases in the p-NF-κB p65 levels, and the HS pre-treatment had the most obvious inhibitory efficacy (Figure 6D).

These results suggest that SAL and hypoxia pre-conditionings synergistically protect rASCs against oxidative injury through anti-oxidant and anti-inflammation mechanisms.

### 3.4 | SAL and hypoxia pre-conditionings show synergistical effects on migration but not proliferation of rASCs under H<sub>2</sub>O<sub>2</sub>-induced oxidative stress

As shown in Figure 7A, BrdU-positive cells represent the cells in DNA-synthetic phase (S phase). The NS, HC and HS pre-treatments significantly increased the proliferation of rASCs, compared to the NC + H<sub>2</sub>O<sub>2</sub> group (Figure 7B). rASCs in the HS + PBS group showed the highest BrdU positivity ratio among each experimental group (Figure 7B).

After the NS, HC or HS pre-treatment followed by the H<sub>2</sub>O<sub>2</sub> treatment, the number of rASCs penetrating the Transwell chamber was respectively  $1.59 \pm 0.09$ ,  $1.71 \pm 0.07$  and  $1.98 \pm 0.08$  folds that of the NC + H<sub>2</sub>O<sub>2</sub> group with statistical significance (Figure 7C,D). Besides, rASCs pre-treated with HS followed by the H<sub>2</sub>O<sub>2</sub> treatment migrated significantly more than the NS + H<sub>2</sub>O<sub>2</sub> and HC + H<sub>2</sub>O<sub>2</sub> groups.

We also determined the expression of Akt, p-Akt, Erk1/2 and p-Erk1/2 using Western blot. The levels of p-Akt and p-Erk1/2 were obviously decreased after the NC pre-treatment followed by the H<sub>2</sub>O<sub>2</sub> treatment (Figure 7E,F). Compared to the NC + H<sub>2</sub>O<sub>2</sub> group, NS + H<sub>2</sub>O<sub>2</sub>, HC + H<sub>2</sub>O<sub>2</sub> and HS + H<sub>2</sub>O<sub>2</sub> significantly increased the levels of p-Akt and p-Erk1/2 with HS + H<sub>2</sub>O<sub>2</sub> group exhibiting higher levels than NS + H<sub>2</sub>O<sub>2</sub> and HC + H<sub>2</sub>O<sub>2</sub> groups.

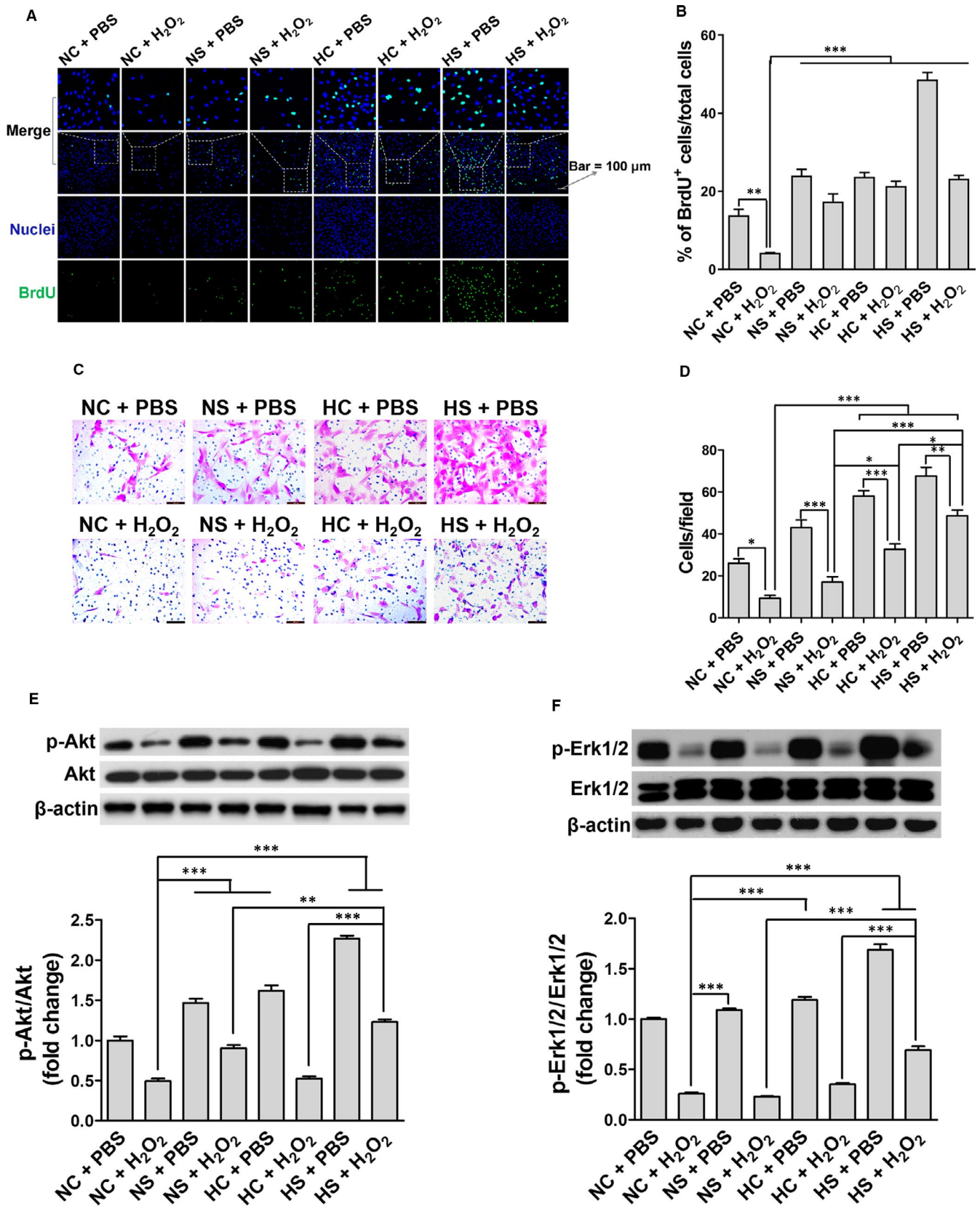


**FIGURE 7** Effects of SAL and hypoxia pre-treatments on cell proliferation, migration and activation of Akt and Erk1/2 after the H<sub>2</sub>O<sub>2</sub> treatment. The cell proliferation was analysed by BrdU incorporation assay (A and B), and the cell migration was measured by Transwell migration assay (C and D). The phosphorylation levels of Akt (E) and Erk1/2 (F) were analysed by Western blot. \**P* < .05, \*\**P* < .01, \*\*\**P* < .001

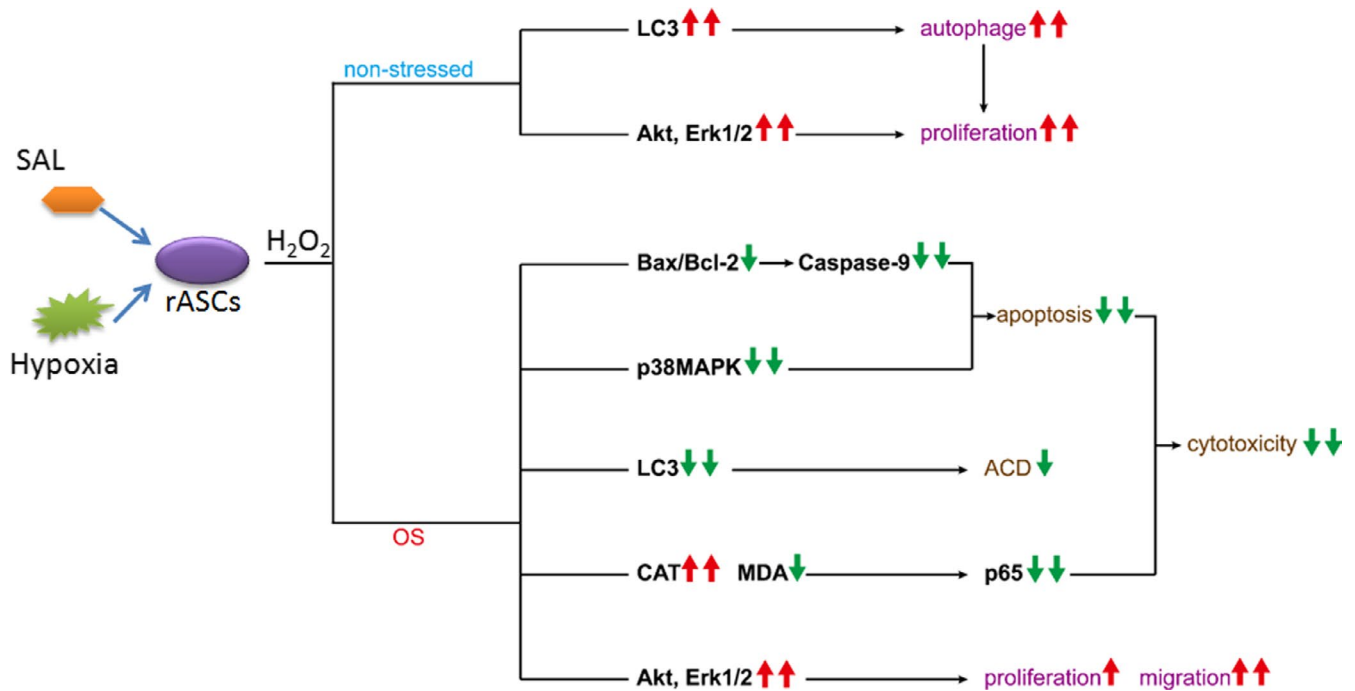


**FIGURE 8** Schematic diagram demonstrates SAL pre-conditioning combined with hypoxia improves the function of rASCs under non-stressed and stressed conditions. OS, oxidative stress

In summary, these results indicate that SAL and hypoxia pre-conditionings enhance the proliferation and migration of rASCs under oxidative stress in association with Akt and Erk1/2 activation, and SAL pre-conditioning has an enhanced potential in improving the migration but not proliferation of hypoxia-pre-conditioned rASCs.

#### 4 | DISCUSSION

This study demonstrated that SAL and hypoxia pre-conditionings synergistically improve ASC function by modulating the proliferation, migration and tolerance against oxidative stress. rASCs cultured with SAL or 5% O<sub>2</sub> exhibited significantly enhanced cell proliferation and autophagic flux, and the effects were enhanced by the combined treatment. Furthermore, H<sub>2</sub>O<sub>2</sub>-induced cell death, excessive oxidative stress and inflammation were attenuated by the pre-treatment with SAL, hypoxia or the both; meanwhile, late-stage autophagy in rASCs was inhibited, and the capacity of proliferation and migration of rASCs were obviously improved. The results of Western blot revealed that Akt, Erk1/2, LC3, NF-κB and apoptosis pathways may be involved in this regulatory mechanism.

Recent studies have revealed that low oxygen tension or hypoxia promotes the survival and function of MSCs.<sup>14,22-24</sup> In addition, pre-conditioning with the components of the traditional Chinese herbs is also a promising strategy.<sup>25-29</sup> Using the cell number counting assay and BrdU incorporation assay, we found that the treatment with SAL or hypoxia (5% O<sub>2</sub>) increased the proliferation capacity and autophagic flux of rASCs under non-stressed conditions, and the combined treatment enhanced these effects (Figure 2). Moreover, up-regulated levels of p-Akt, p-Erk1/2 and LC3-II/LC3-I were

observed after the individual or combined treatment, which may explain the mechanisms of SAL and hypoxia pre-conditionings involved in the proliferation of rASCs (Figure 3). These findings suggest that SAL pre-conditioning combined with hypoxia pre-conditioning allows the production of numerous rASCs from a few donor cells.

Accumulating evidence has demonstrated the poor survival and retention of transplanted cells *in vivo*, due to the properties of cell themselves and the extremely hostile microenvironment in the infarct tissues.<sup>31,32</sup> A prior study has noticed the importance that survival, proliferation and migration of implanted stem cells within the cardiac environment are crucial to the therapeutic efficacy of stem cell transplantation.<sup>33</sup> Thus, extending the lifespan of stem cells is required for improving their survival under ischaemic conditions. Oxidative stress and inflammatory responses following infarction are implicated in the pathogenesis of stem cell dysfunction.<sup>34</sup> Oxidative stress-induced ROS have been shown to cause cell death and cellular ageing in different cell types.<sup>35,36</sup> In response to the infarct microenvironment, the stressed stem cells release various immunomodulatory signalling factors, including both pro-inflammatory and anti-inflammatory cytokines, thereby displaying their immunomodulatory roles.<sup>35,37</sup>

As one of the common ROS, H<sub>2</sub>O<sub>2</sub> can easily cross the plasma membrane and stimulate consecutive reactions leading to cell apoptosis and inflammatory responses.<sup>36</sup> Our present results show that the H<sub>2</sub>O<sub>2</sub> treatment led to increased cytotoxicity, apoptosis, late-stage autophagy, oxidative stress and NF-κB activation in rASCs, which were alleviated by the SAL or hypoxia pre-treatment; moreover, the combined pre-treatment with SAL and hypoxia has synergistic effects (Figures 4-6). The results imply that SAL pre-conditioning combined with hypoxia pre-conditioning can

validly attenuate H<sub>2</sub>O<sub>2</sub>-mediated cell death and inflammatory responses following the initial oxidative stress, thus may promote stem cells to exert immunosuppressive function and tissue repair activity.

In the current study, cell proliferation and migration of rASCs under H<sub>2</sub>O<sub>2</sub>-induced oxidative stress were respectively observed by BrdU incorporation assay and Transwell migration assay. The results showed that the pre-treatment with SAL, hypoxia or the both is key to maintaining cell proliferation and migration of rASCs under oxidative environment; the combined pre-treatment showed the best effects on cell migration (Figure 7A-D). Lots of evidences have shown that Akt and Erk1/2 signalling is involved in the viability, proliferation and migration of stem cells including MSCs.<sup>38-43</sup> Moreover, the results of Western blot confirmed that Akt and Erk1/2 signalling contributes to proliferation and migration of pre-conditioned rASCs under oxidative stress (Figure 7E,F). These findings suggest that SAL pre-conditioning may further facilitate the self-renewal divisions and homing ability of hypoxia-pre-conditioned stem cells in the ischaemic micro-environment.

Autophagy, an intracellular degradation and recycling of cytoplasmic contents, plays a double-edged sword effect on cell fate.<sup>13</sup> Several studies have reported that autophagy is involved in the survival and proliferation of MSCs.<sup>44-46</sup> However, recent reports have indicated that chronic stress and ROS can induce ACD of stem cells.<sup>16-21</sup> In the present study, rASCs were transfected with LV which mediated stable expression of stubRFP-sens-GFP-LC3 in rASCs. During autophagy, LC3-I is converted to an autophagosome-associating form called LC3-II.<sup>47</sup> Sens-GFP is an acid-sensitive protein, while stub-RFP is a stable fluorescent protein unaffected by the internal environment of lysosome. Thus, the yellow dots (overlays of red and green channels) and red dots respectively represent autophagosomes and autolysosomes. Here, we found the SAL, hypoxia and combined treatments displayed substantial increase in cell proliferation and autophagic flux in rASCs, suggesting autophagy may be beneficial to the survival and proliferation of stem cells under non-stressed conditions (Figure 2E,F). Interestingly, we also found H<sub>2</sub>O<sub>2</sub> induced cytotoxicity along with simultaneous up-regulation of autophagosomes/autolysosomes in rASCs; in contrast, the hypoxia and combined pre-treatments reversed the up-regulation of autolysosomes under oxidative stress (Figure 4A,E,F). These findings indicate that stem cell growth and survival under non-stressed and stressed conditions are differentially regulated by autophagy. The SAL and hypoxia treatments can facilitate cytoprotective autophagy in non-stressed cells by up-regulating early- and late-stage autophagy, while the hypoxia and combined pre-treatments eliminate ACD of stressed cells by attenuating the late-stage autophagy, suggesting differential regulatory mechanisms may be involved in the process of SAL and hypoxia pre-conditionings modulating autophagic flux under different conditions. Hence, further investigations will need to focus on the underlying mechanisms of how SAL and hypoxia pre-conditionings counterbalance the autophagic activity of stem cells.

## 5 | CONCLUSIONS

In conclusion, our results shed light on a better understanding of the effects and mechanisms of SAL pre-conditioning combined with hypoxia pre-conditioning on rASC function (Figure 8). The present study clearly demonstrates for the first time that SAL pre-conditioning further improves the function of hypoxia-pre-conditioned rASCs by enhancing the proliferation, migration and tolerance against oxidative stress. Importantly, we partly identified the mechanisms underlying the multi-target effects of SAL and hypoxia pre-conditionings on rASC function. This study also suggests that SAL pre-conditioning combined with hypoxia may facilitate a higher therapeutic capacity of ASCs in post-ischaemic repair.

## ACKNOWLEDGEMENTS

We thank Prof. Jing Zheng from University of Wisconsin-Madison for editing the English text of this manuscript. This paper was supported by the National Natural Science Foundation of China (81700269, 81970056), Southern Marine Science and Engineering Guangdong Laboratory Zhanjiang (ZJW-2019-007), Natural Science Foundation of Guangdong Province (2019A1515011925), the Project of Guangdong Provincial Bureau of Traditional Chinese Medicine (20182068), the Competitive Key Scientific and Technological Program of Zhanjiang Municipal Financial Fund (2018A01023) and the Stem Cell Preclinical Research Projects of the Affiliated Hospital of Guangdong Medical University (2018PSSC004).

## CONFLICTS OF INTEREST

The authors declare that there is no conflict of interests regarding the publication of the paper.

## AUTHOR CONTRIBUTION

**Yuan He:** Data curation (equal); Formal analysis (equal); Methodology (equal); Writing-original draft (equal); Writing-review & editing (equal). **Mudi Ma:** Data curation (equal); Formal analysis (equal); Investigation (equal); Methodology (equal). **Yiguang Yan:** Data curation (equal); Methodology (equal). **Can Chen:** Funding acquisition (equal); Project administration (equal); Validation (equal). **Hui Luo:** Funding acquisition (equal); Project administration (equal). **Wei Lei:** Funding acquisition (equal); Project administration (equal); Writing-review & editing (equal).

## DATA AVAILABILITY STATEMENT

The data that support the findings of this study are available from the corresponding author upon reasonable request.

## ORCID

Wei Lei  <https://orcid.org/0000-0002-4033-4799>

## REFERENCES

1. De Ugarte DA, Morizono K, Elbarbary A, et al. Comparison of multi-lineage cells from human adipose tissue and bone marrow. *Cells Tissues Organs*. 2003;174(3):101-109.

2. Nakagami H, Morishita R, Maeda K, Kikuchi Y, Ogihara T, Kaneda Y. Adipose tissue-derived stromal cells as a novel option for regenerative cell therapy. *J Atheroscler Thromb*. 2006;13(2):77-81.
3. Fraser JK, Schreiber R, Strem B, et al. Plasticity of human adipose stem cells toward endothelial cells and cardiomyocytes. *Nat Clin Pract Cardiovasc Med*. 2006;3(Suppl 1):S33-S37.
4. Strem BM, Zhu M, Alfonso Z, et al. Expression of cardiomyocytic markers on adipose tissue-derived cells in a murine model of acute myocardial injury. *Cytotherapy*. 2005;7(3):282-291.
5. Yang D, Wang W, Li L, et al. The relative contribution of paracrine effect versus direct differentiation on adipose-derived stem cell transplantation mediated cardiac repair. *PLoS One*. 2013;8(3):e59020.
6. Mazo M, Hernández S, Gavira JJ, et al. Treatment of reperfused ischemia with adipose-derived stem cells in a preclinical Swine model of myocardial infarction. *Cell Transplant*. 2012;21(12):2723-2733.
7. Tongers J, Losordo DW, Landmesser U. Stem and progenitor cell-based therapy in ischaemic heart disease: Promise, uncertainties, and challenges. *Eur Heart J*. 2011;32(10):1197-1206.
8. Chacko SM, Ahmed S, Selvendiran K, Kuppusamy ML, Khan M, Kuppusamy P. Hypoxic preconditioning induces the expression of pro-survival and proangiogenic markers in mesenchymal stem cells. *Am J Physiol Cell Physiol*. 2010;299(6):C1562-1570.
9. Penn MS, Mangi AA. Genetic enhancement of stem cell engraftment, survival, and efficacy. *Circ Res*. 2008;102(12):1471-1482.
10. Terrovitis JV, Smith RR, Marbán E. Assessment and optimization of cell engraftment after transplantation into the heart. *Circ Res*. 2010;106(3):479-494.
11. Forte G, Pietronave S, Nardone G, et al. Human cardiac progenitor cell grafts as unrestricted source of supernumerary cardiac cells in healthy murine hearts. *Stem Cells*. 2011;29(12):2051-2061.
12. Wagner W, Bork S, Horn P, et al. Aging and replicative senescence have related effects on human stem and progenitor cells. *PLoS One*. 2009;4(6):e5846.
13. Shintani T, Klionsky DJ. Autophagy in health and disease: a double-edged sword. *Science*. 2004;306(5698):990-995.
14. Liu J, Hao J, Huang H, et al. Hypoxia regulates the therapeutic potential of mesenchymal stem cells through enhanced autophagy. *Int J Low Extrem Wounds*. 2015;14(1):63-72.
15. Yonekawa T, Thorburn A. Autophagy and cell death. *Essays Biochem*. 2013;55:105-117.
16. Ji ST, Kim YJ, Jung SY, et al. Oleuropein attenuates hydrogen peroxide-induced autophagic cell death in human adipose-derived stem cells. *Biochem Biophys Res Commun*. 2018;499(3):675-680.
17. Ou X, Lee MR, Huang X, Messina-Graham S, Broxmeyer HE. SIRT1 positively regulates autophagy and mitochondria function in embryonic stem cells under oxidative stress. *Stem Cells*. 2014;32(5):1183-1194.
18. Ha S, Ryu HY, Chung KM, Baek SH, Kim EK, Yu SW. Regulation of autophagic cell death by glycogen synthase kinase-3 $\beta$  in adult hippocampal neural stem cells following insulin withdrawal. *Mol Brain*. 2015;8:30.
19. Chung KM, Park H, Jung S, et al. Calpain determines the propensity of adult hippocampal neural stem cells to autophagic cell death following insulin withdrawal. *Stem Cells*. 2015;33(10):3052-3064.
20. Chung KM, Jeong EJ, Park H, An HK, Yu SW. Mediation of autophagic cell death by type 3 ryanodine receptor (RyR3) in adult hippocampal neural stem cells. *Front Cell Neurosci*. 2016;10:116.
21. Yeo BK, Hong CJ, Chung KM, et al. Valosin-containing protein is a key mediator between autophagic cell death and apoptosis in adult hippocampal neural stem cells following insulin withdrawal. *Mol Brain*. 2016;9:31.
22. Kakudo N, Morimoto N, Ogawa T, Taketani S, Kusumoto K. Hypoxia enhances proliferation of human adipose-derived stem cells via HIF-1 $\alpha$  activation. *PLoS One*. 2015;10(10):e0139890.
23. Stubbs SL, Hsiao ST, Peshavariya HM, Lim SY, Dusting GJ, Dilley RJ. Hypoxia preconditioning enhances survival of human adipose-derived stem cells and conditions endothelial cells in vitro. *Stem Cells Dev*. 2012;21(11):1887-1896.
24. Liu J, Hao H, Xia L, et al. Hypoxia pretreatment of bone marrow mesenchymal stem cells facilitates angiogenesis by improving the function of endothelial cells in diabetic rats with lower ischemia. *PLoS One*. 2015;10(5):e0126715.
25. Choe KI, Kwon JH, Park KH, et al. The antioxidant and anti-inflammatory effects of phenolic compounds isolated from the root of *Rhodiola sachalinensis* A. BOR. *Molecules*. 2012;17(10):11484-11494.
26. Bai H, Wang CB, Ma XH, et al. Effects of salidroside on proliferation of bone marrow mesenchymal stem cells. *J Exp Hematol*. 2014;22(4):1072-1077.
27. Wei YP, Bai H, Sun YQ, Bao S, Xi R, Liu L. Effect of salidroside on apoptosis of bone marrow mesenchymal stem cells induced by ara-C. *Zhongguo J Exp Hematol*. 2013;21(6):1572-1577.
28. Zhang XS, Zhu BD, Hung XQ, Chen YF. Effect of salidroside on bone marrow cell cycle and expression of apoptosis-related proteins in bone marrow cells of bone marrow depressed anemia mice. *J Sichuan Univ (Med Sci Ed)*. 2005;36(6):820-823, 846.
29. Li X, Erden O, Li L, Ye Q, Wilson A, Du W. Binding to WGR domain by salidroside activates PARP1 and protects hematopoietic stem cells from oxidative stress. *Antioxid Redox Signal*. 2014;20(12):1853-1865.
30. Dong Y, Cui P, Li Z, Zhang S. Aging asymmetry: systematic survey of changes in age-related biomarkers in the annual fish *Nothobranchius guentheri*. *Fish Physiol Biochem*. 2017;43(2):309-319.
31. Dai G, Xu Q, Luo R, et al. Atorvastatin treatment improves effects of implanted mesenchymal stem cells: meta-analysis of animal models with acute myocardial infarction. *BMC Cardiovasc Disord*. 2015;15:170.
32. Peng Y, Huang S, Wu Y, et al. Platelet rich plasma clot releasate preconditioning induced PI3K/AKT/NF $\kappa$ B signaling enhances survival and regenerative function of rat bone marrow mesenchymal stem cells in hostile microenvironments. *Stem Cells Dev*. 2013;22(24):3236-3251.
33. Cao F, Lin S, Xie X, et al. In vivo visualization of embryonic stem cell survival, proliferation, and migration after cardiac delivery. *Circulation*. 2006;113(7):1005-1014.
34. Frangogiannis NG. The inflammatory response in myocardial injury, repair, and remodeling. *Nat Rev Cardiol*. 2014;11(5):255-265.
35. Rameshwar P, Qiu H, Vatner SF. Stem cells in cardiac repair in an inflammatory microenvironment. *Minerva Cardioangiol*. 2010;58(1):127-146.
36. Lugin J, Rosenblatt-Velin N, Parapanov R, Liaudet L. The role of oxidative stress during inflammatory processes. *Biol Chem*. 2014;395(2):203-230.
37. Patel SA, Sherman L, Munoz J, Rameshwar P. Immunological properties of mesenchymal stem cells and clinical implications. *Arch Immunol Ther Exp (Warsz)*. 2008;56(1):1-8.
38. Bai T, Liu F, Zou F, et al. Epidermal growth factor induces proliferation of hair follicle-derived mesenchymal stem cells through epidermal growth factor receptor-mediated activation of ERK and AKT signaling pathways associated with upregulation of cyclin D1 and downregulation of p16. *Stem Cells Dev*. 2017;26(2):113-122.
39. Choi NY, Kim JY, Hwang M, et al. Atorvastatin rejuvenates neural stem cells injured by oxygen-glucose deprivation and induces neuronal differentiation through activating the PI3K/Akt and ERK pathways. *Mol Neurobiol*. 2019;56(4):2964-2977.
40. Tsai KS, Kao SY, Wang CY, Wang YJ, Wang JP, Hung SC. Type I collagen promotes proliferation and osteogenesis of human mesenchymal stem cells via activation of ERK and Akt pathways. *J Biomed Mater Res A*. 2010;94(3):673-682.
41. Park JH, Han HJ. Caveolin-1 plays important role in EGF-induced migration and proliferation of mouse embryonic stem cells:

- involvement of PI3K/Akt and ERK. *Am J Physiol Cell Physiol.* 2009;297(4):C935-C944.
42. Ryu CH, Park SA, Kim SM, et al. Migration of human umbilical cord blood mesenchymal stem cells mediated by stromal cell-derived factor-1/CXCR4 axis via Akt, ERK, and p38 signal transduction pathways. *Biochem Biophys Res Commun.* 2010;398(1):105-110.
43. Guo Y, Chen S, Xu L, et al. Decellularized and solubilized pancreatic stroma promotes the in vitro proliferation, migration and differentiation of BMSCs into IPCs. *Cell Tissue Bank.* 2019;20(3):389-401.
44. Phadwal K, Watson AS, Simon AK. Tightrope act: autophagy in stem cell renewal, differentiation, proliferation, and aging. *Cell Mol Life Sci.* 2013;70(1):89-103.
45. Guan JL, Simon AK, Prescott M, et al. Autophagy in stem cells. *Autophagy.* 2013;9(6):830-849.
46. Lee HJ, Ryu JM, Jung YH, Oh SY, Lee SJ, Han HJ. Novel pathway for hypoxia-induced proliferation and migration in human mesenchymal stem cells: involvement of HIF-1 $\alpha$ , FASN, and mTORC1. *Stem Cells.* 2015;33(7):2182-2195.
47. Kabeya Y, Mizushima N, Yamamoto A, Oshitani-Okamoto S, Ohsumi Y, Yoshimori T. LC3, GABARAP and GATE16 localize to autophagosomal membrane depending on form-II formation. *J Cell Sci.* 2004;117(Pt 13):2805-2812.

**How to cite this article:** He Y, Ma M, Yan Y, Chen C, Luo H, Lei W. Combined pre-conditioning with salidroside and hypoxia improves proliferation, migration and stress tolerance of adipose-derived stem cells. *J Cell Mol Med.* 2020;24:9958-9971. <https://doi.org/10.1111/jcmm.15598>